Monatshefte für Chemie 110, 1153—1170 (1979)

Monatshefte für Chemie

Transition Metal—Chalcogen Systems, VII.: The Iron—Selenium Phase Diagram

Wilfried Schuster, Helga Mikler, and **Kurt L. Komarek** *

Institute of Inorganic Chemistry, University of Vienna, A-1090 Vienna, Austria

(Received 9 January 1979. Accepted 5 February 1979)

The binary iron—selenium system was investigated by thermoanalytical and isopiestic methods and by X-ray analysis. Combining all results a temperature-concentration diagram was constructed from 20 to 66 at% Se and between 623 and 1,373 K. Two compounds and several NiAs-related structures could be identified. Tetragonal β-FeSe with a narrow stability range between 49.0 and 49.4 at% Se at 653 K decomposes by a peritectoid reaction at 730 K. The NiAs-related structures $Fe_{1-x}Se$ have a wide range of homogeneity from 51.5 to 58.5 at% Se at 823 K. The iron-rich hexagonal δ-phase extends from 51.5 to 54.3 at% Se, and transforms to a high temperature modification δ′ of unknown structure with a maximum transformation temperature of 1,338 K at 52.8 at% Se. The congruent melting point of the δ′-phase is located at 1,351 K and 52.0 at% Se. At ≈ 54 at% Se the δ-phase undergoes a λ-transformation to the monoclinic γ′-phase which is stable between 54.3 and 54.6 at% Se. Between 54.6 and 56.4 at% Se two very similar monoclinic phases coexist: the γ′- and the γ-phase with similar *a*- and *b*-axes but a simple *c*′- and a double *c*-axis, resp. Between 56.4 and 58.5 at% Se the γ-phase is stable. Orthorhombic ε-$FeSe_2$ (marcasite structure) with a very narrow range of homogeneity at 66.6 at% Se decomposes peritectically at 858 K. On the iron-rich side there are three invariant equilibria at high temperatures: a monotectic at 1,234 K and 46.5 at% Se, a eutectic at 1,215 K and 5.5 at% Se, and a eutectoid at 1,149 K. On the selenium-rich side there is a eutectoid at 1,122 K, a monotectic at 1,068 K and 71.5 at% Se, and a peritectic at 1,001 K.

(Keywords: Chalcogen systems; Iron—selenium; Phase diagram, Fe—Se*)*

Übergangsmetall—Chalcogen-Systeme, 7. Mitt.: Das Eisen—Selen-Phasen-Diagramm

Das Zweistoffsystem Eisen—Selen wurde thermisch, röntgenographisch und isopiestisch untersucht. Aus den Ergebnissen konnte das T-x-Zustandsdiagramm für den Bereich von 20 bis 66 At% Se und von 623 bis 1 373 K erstellt werden. Zwei Verbindungen und einige NiAs-ähnliche Strukturen konnten identifiziert werden. Die tetragonale β-Phase FeSe besitzt bei 653 K eine

0026-9247/79/0110/1153/$ 03.60

schmale Phasenbreite von 49,0 bis 49,4 At% Se und zerfällt peritektoidisch bei 730 K. Die NiAs-ähnlichen Strukturen $Fe_{1-x}Se$ haben bei 823 K einen breiten Homogenitätsbereich von 51,5 bis 58,5 At% Se. Die eisenreiche hexagonale δ-Phase reicht von 51,5 bis 54,3 At% Se und wandelt sich bei 1338 K und 52,8 At% Se in eine Hochtemperaturmodifikation mit unbekannter Struktur, die δ'-Phase, um, deren kongruenter Schmelzpunkt bei 52,0 At% Se und 1351 K liegt. Bei etwa 54 At% Se geht das hexagonale Gitter infolge einer λ-Umwandlung in die monokline γ'-Phase über, welche von 54,3 bis 54,6 At% Se reicht. Zwischen 54,6 und 56,4 At% Se liegt ein Zweiphasengebiet von zwei sehr ähnlichen monoklinen Phasen: die γ'- und die γ-Phase mit ähnlichen *a*- und *b*-Parametern, aber einfacher *c*'- bzw. doppelter *c*-Achse. Die monokline γ-Phase befindet sich zwischen 56,4 und 58,5 At% Se. Die orthorhombische ε-Phase $FeSe_2$ mit Markasitstruktur mit einem sehr engen Homogenitätsbereich bei 66,6 At% Se zerfällt peritektisch bei 858 K. An der eisenreichen Seite gibt es bei höheren Temperaturen drei invariante Gleichgewichte: ein Eutektikum bei 5,5 At% Se und 1215 K, ein Monotektikum bei 46,5 At% Se und 1234 K und ein Eutektoid bei 1149 K. An der selenreichen Seite existiert bei 71,5 At% Se und 1068 K ein Monotektikum, bei 1122 K ein Eutektoid und bei 1001 K ein Peritektikum.

Introduction

In continuation of previous work on transition metal—chalcogen systems[1–10] thermoanalytical, X-ray, and isopiestic investigations were carried out in the binary iron—selenium system.

In one of the first studies *Hägg* and *Kindström*[11] described two types of structures: a tetragonal phase FeSe with PbO-structure and a NiAs-related phase with a wide range of homogeneity showing a transformation from hexagonal to monoclinic symmetry. A third compound, $FeSe_2$, has according to *Tengnér*[12] the orthorhombic marcasite structure. Investigations by *Haraldsen* and *Grønvold*[13] confirmed the existence of these three phases and their stability ranges. According to these earlier investigations three compounds with different structures are present in the iron—selenium system:

1. The tetragonal monoselenide, $Fe_{1.04}Se$ (49.02 at% Se) with additional iron atoms on interstitial lattice sites, with the PbO-structure (B 10-type). The lattice parameters of this phase were determined by *Hägg* and *Kindström*[11], *Grønvold*[14], and *Reddy* and *Chetty*[15]. Tetragonal $Fe_{1.04}Se$ transforms by a peritectoid reaction into the NiAs-structure according to *Hägg* and *Kindström*[11], *Tröften* and *Kullerud*[16], and *Kullerud*[17] at 300° to 600 °C, 335°, and 380 °C, resp. Alloys which were quenched from temperatures slightly below the melting point still contained the tetragonal phase together with the NiAs-phase as shown by X-ray studies of *Reddy* and *Chetty*[15] and of *Gorokh* et al.[18]. Measurements of heat capacity and high temperature X-ray studies by *Grønvold*[14] established the transformation of the tetragonal PbO-phase into a NiAs-related phase and iron by a peritectoid reaction at 457 °C.

Tsuji et al.[19] confirmed by *Mössbauer* spectroscopy the transformation temperature with 458 °C; these authors assumed for $Fe_{1.04}Se$ on anti-PbO-structure.

2. The phases with NiAs-related structure, described by the general formula $Fe_{1-x}Se$, have at 600 °C a wide range of homogeneity between ≈ 51 and ≈ 59 at% Se. Compositions referred to Fe_7Se_8 (53.3 at% Se) have the hexagonal NiAs-structure, those expressed by Fe_3Se_4 (57.1 at% Se) show monoclinic deformation. Both variants of the NiAs-structure are characterized by iron vacancies. The lattice parameters of the $Fe_{1-x}Se$ phase have been described in numerous publications[11, 14, 15, 20, 21]. *Hägg* and *Kindström*[11] noticed in the entire range of the NiAs-related phases a steady decrease of the lattice parameters with increasing Se-concentration; at 53 at% Se the orthohexagonal cell became monoclinically distorted with a maximum deformation at 55 to 56 at% Se which decreased again towards the phase boundary at 57.5 at% Se. In the hexagonal range of $Fe_{1-x}Se$ (Fe_7Se_8) the results of *Hägg* and *Kindström*[11] were confirmed by *Grønvold*[14], and *Reddy* and *Chetty*[15].

For monoclinic $Fe_{1-x}Se$ (Fe_3Se_4) *Okazaki* and *Hirakawa*[20] reported in difference to *Hägg* and *Kindström*[11] a doubling of the *c*-axis of the monoclinically distorted lattice which can be explained by an ordering of the vacancies in every other metal atom layer parallel to the *a*-*b* plane. These lattice parameters were confirmed by neutron diffraction studies of *Andresen*[21] while *Reddy* and *Chetty*[15] based their evaluation on the simple *c*-axis. *Okazaki* and *Hirakawa*[20] and *Okazaki*[22, 23] also investigated the structural changes of Fe_7Se_8 at lower temperatures. Slowly cooled alloys showed below 240 °C a triclinic superstructure of the NiAs-type with an ordered arrangement of iron vacancies characterized by a fourfold *c*-axis of the basic hexagonal lattice. This 4 *c*- or low temperature structure transforms between 240° and 298 °C into still another hexagonal superstructure, the 3 *c*- or high temperature structure, with a threefold *c*-axis of the basic hexagonal lattice. In the range between 360° and 375 °C another rearrangement of the iron vacancies was assumed so that above this temperature only lines of the simple basic hexagonal lattice with some remaining lines of the 3 *c*-superstructure were found. Structures of this kind are designated as NiAs-related structures; the ideal NiAs-structure is not realized in the iron—selenium system. The ordered arrangement of iron vacancies of the hexagonal 3 *c*-superstructure was confirmed by neutron diffraction studies of *Andresen* and *Leciejewicz*[24] on specimens which were slowly cooled from 600 °C.

Heat capacities published by *Grønvold* and *Westrum*[25] and by *Grønvold*[14, 26] show a temperature dependence characteristic for λ-type

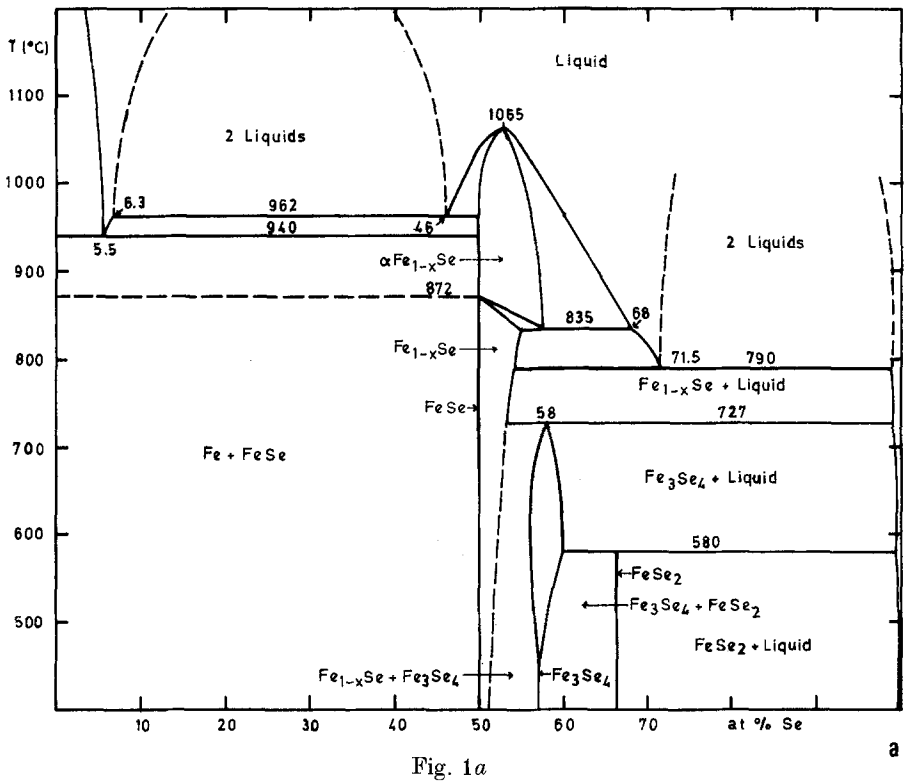

Fig. 1*a*

Fig. 1. Iron—Selenium phase diagram (literature data). *a Kullerud*[17], *b Dutrizac* et. al.[28], *c Svendsen*[27]

transformations. In Fe_7Se_8 two λ-transformations were found: one with a maximum of the heat capacity at 178 °C was explained by the change from ferri- to paramagnetism, the other with a maximum at 365 °C could be related to the structural transformation of the 3*c*-superstructure into the basic hexagonal lattice as previously described[20]. Fe_3Se_4 also exhibits two λ-transitions: the first at 34 °C was ascribed to a magnetic ordering process, the second at 704 °C was caused by a structural change from ordered to disordered iron vacancies accompanied by a change in symmetry from monoclinic to hexagonal. The congruent melting point of the hexagonal $Fe_{1-x}Se$-phase was reported by *Svendsen*[27] to be 1,065 °C at 53.6 at% Se. This value was confirmed by other authors[16, 17, 28, 29]. *Kullerud*[17] described the existence of a high temperature modification of the hexagonal NiAs-related phase above 872 °C in the range between ≈ 50 and 56 at% Se. *Dutrizac* et al.[28] and

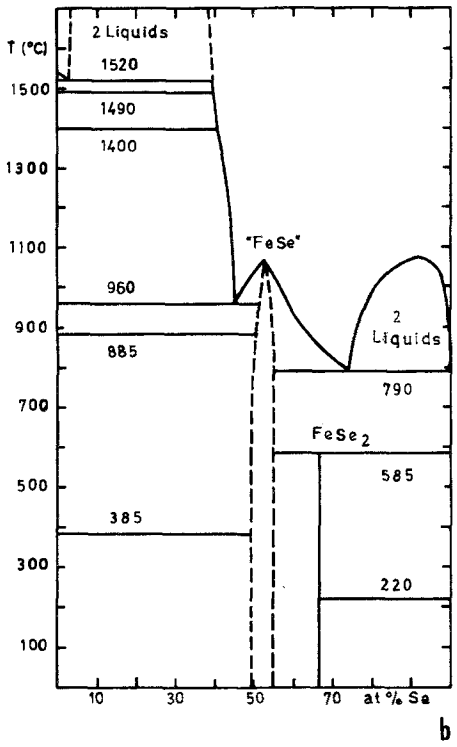

Fig. 1*b*

Svendsen[27] also reported thermal arrests at 885° and 872 °C, resp. According to *Mann* and *van Vlack*[30] the hexagonal $Fe_{1-x}Se$-phase transforms at 868 °C into another not further identified phase.

3. $FeSe_2$, the phase richest in selenium, has the marcasite (C 18-type) structure with a narrow range of homogeneity at 66.6 at% Se. Lattice parameters calculated by *Tengnér*[12] and *Fischer*[29] were confirmed by *Grønvold* and *Westrum*[31], *Kjekshus* et al.[32] and *Reddy* and *Chetty*[15]. The incongruent melting point of $FeSe_2$ at 585 °C as reported by *Svendsen*[27,33] was also found by other authors[16,17,28,34,35]. *Bither* et al.[36] described the high pressure-high temperature synthesis of a $FeSe_2$ modification with pyrite structure.

The first attemps to construct the binary iron—selenium phase diagram go back to *Hirone* et al.[37], and *Hirone* and *Chiba*[38]. Based on thermal, X-ray and magnetic measurements these authors tried to draw a partial phase diagram between 48.8 and 56.0 at% Se in the temperature range from 100° to 400 °C. *Tröften* and *Kullerud*[16], and

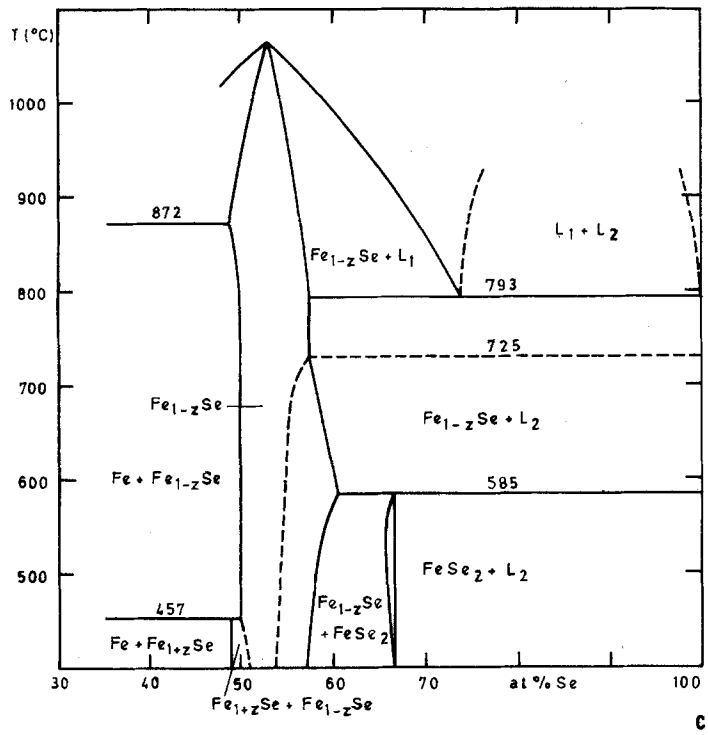

Fig. 1c

Serre and *Druilhe*[39] extended the temperature range up to the melting point of the NiAs-phase. *Kullerud*[17], *Dutrizac* et al.[28] and *Svendsen*[27] published more or less complete but rather different versions of the iron—selenium phase diagram as can be seen in Fig. 1. The selenium-rich parts of the diagrams are very similar and show but minor deviations: the incongruent melting point of $FeSe_2$, the λ-transformation of Fe_3Se_4, the monotectic at 793 °C, and the congruent melting point of the $Fe_{1-x}Se$-phase are in substantial agreement. Large discrepancies, however, are found in the region of the NiAs-phase $Fe_{1-x}Se$ and in the iron-rich part of the phase diagram.

In the present investigation the iron—selenium phase diagram was therefore studied to resolve these differences. The system was investigated in detail between 20 and 66 at% Se by X-ray analysis and thermoanalytical measurements. For the determination of phase boundaries, especially in the range of the NiAs-related structures, isopiestic experiments were also employed.

Experimental Procedure

As starting materials selenium shots (99.999% Se, ASARCO, New York, U.S.A.), thin iron sheet (99.9% Fe, Ferrovac E, Vacuum Metals Corp., Syracuse, U.S.A.), and iron wire with a diameter of 0.2 mm (99.9% Fe, Allied Chemical Dye Corp., U.S.A.) were employed. The DTA- and X-ray specimens were prepared from the iron sheet, the iron wire was used for the isopiestic experiments. Sheet and wire were mechanically cleaned and degreased with acetone. Samples (3 to 5 g) were weighed on a microbalance to within $\pm$ 0.05 mg, and placed into quartz capsules which were then evacuated to 10^{-1} to 10^{-2} Pa, flushed with Ti-gettered argon, and finally sealed under vacuum. The quartz-capsules were inserted into a larger quartz tube which was also sealed under vacuum to prevent oxidation of the specimens since selenides tend to crack the capsules on cooling. The encapsulated samples were then heated in an electric furnace at 1,000° to 1,100 °C for about 20 days.

Specimens for X-ray analysis were comminuted, the powder heated in evacuated and sealed quartz capsules three to ten weeks at the desired temperature, and then quenched in ice water. X-ray measurements were made with a Kristalloflex 4 (Fa. Siemens, Karlsruhe, BRD) in *Debye-Scherrer* cameras with diameters of 57.29 and 114.58 mm using filtered Co-$K\alpha$-radiation. For DTA-measurements a fully automated apparatus was available[1]. Specimens ($\sim$ 3 g) and the reference metal (99.9% Cr) were sealed in thin-walled quartz vessels with reentrant nipples at the bottom for the thermocouple junctions. Temperature and temperature difference were measured with Pt/Pt-10% Rh thermocouples which were calibrated at the melting points of high purity Cd, Zn, Sb, and Ag.

As the composition of the specimens the starting composition was taken. In several alloys the iron content was checked by complexometrie titration[40]. The samples were dissolved in aqua regia, excess HNO_3 was removed by evaporation, and the resulting solution diluted with distilled water to a well-defined volume. To a measured part of the volume standard acetate buffer solution ($pH = 4.62$) was added to give a $pH = 2.0$, and the solution titrated with 0.05*M-EDTA* with sulfosalicylic acid as indicator. The analytical results agreed with the nominal composition within $\pm$ 0.5%.

Results and Discussion

The results of the DTA-measurements are listed in Tab. 1, phase boundaries obtained from isopiestic studies[41] are shown in Tab. 2. Using the data of the present investigation and results published by other authors the phase diagram in Fig. 2 was constructed. To elucidate the complicated phase relationship in the middle part of the system an enlarged partial diagram for the range from 47.0 to 62.5 at% Se with the most important experimental points is presented in Fig. 3.

On the iron-rich side X-ray analysis of samples from 25 to 49 at% Se at 653 K revealed the two-phase field of tetragonal β-FeSe and α-Fe. At 823 K β-FeSe was found together with hexagonal δ-$Fe_{1-x}Se$. Only in a few X-ray films lines of α-Fe could be detected in addition to those of the other two phases. In most cases the tetragonal phase together with

Table 1. *Thermal effects by DTA*

Composition at% Se	Liquidus K	Solidus K	Invariant arrests K							
20.0	—	—	1234	1213	1148	—	—	—	—	750 h 667 c
25.0	—	—	1235	1215	1149	—	—	—	—	747 h 674 c
35.0	—	—	1234	1215	1148	—	—	—	—	751 h 675 c
47.0	1251	—	1237	1215	1148	—	—	—	—	752 h 674 c
48.0	1277	—	1235	1215	1147	—	—	—	—	748 h 673 c
48.5	1285	—	1233	1216	1149	—	—	—	—	748 h 677 c
49.0	1303	—	1234	1215	1149	—	—	—	—	736 h 672 c
49.5	1310	1274	—	—	—	—	—	—	—	738 h 680 c
51.0	1338	1326	—	—	—	—	—	—	—	—
52.5	1349	—	—	—	—	—	—	—	—	—
53.0	1343	—	—	—	—	—	—	—	—	—
53.6	1341	—	—	—	—	—	—	—	—	—
54.5	1333	—	—	—	—	—	—	—	—	—
55.5	1321	1305	—	—	—	—	—	—	—	—
56.5	1309	1293	—	—	—	—	—	—	—	—
57.0	1301	1284	—	—	—	1120	—	—	—	—
57.5	1291	1276	—	—	—	1124	—	—	—	—
60.5	1263	1214	—	—	—	1122	1068	1001	—	—
61.5	1228	1178	—	—	—	1122	1067	1001	858	—
62.0	1234	—	—	—	—	1123	1068	1001	858	—
66.0	1155	—	—	—	—	1119	1069	1002	858	—

Composition at% Se	Other effects K					
49.5	1220	1165	1142	—	—	—
51.0	—	1286	—	—	—	685
52.5	—	1332	—	—	—	—
53.0	—	1333	—	—	—	—
53.6	—	1312	—	—	—	—
54.5	1306	1271	—	781	—	—
55.5	—	1209	—	886	—	—
56.5	1258	1145	—	945	—	—
57.0	1250	—	1113	969	946	—
57.5	1248	—	1104	986	979	—
60.5	1171	—	—	—	—	—
61.5	1136	—	—	—	—	—

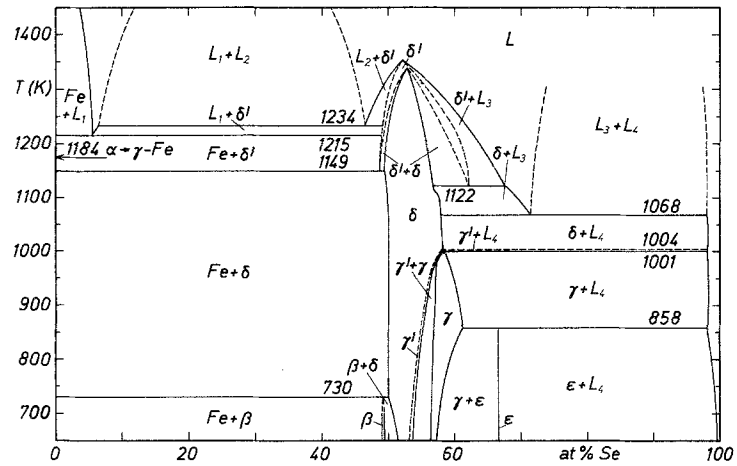

Fig. 2. Iron—Selenium phase diagram (present work)

Table 2. *Phase boundaries from isopiestic experiments*

Composition at% Se	Temperature of the tieline K	Composition at% Se
54.70 $\gamma'/(\gamma'+\gamma)$	808	56.70 $(\gamma'+\gamma)/\gamma$
54.90 $\gamma'/(\gamma'+\gamma)$	833	56.70 $(\gamma'+\gamma)/\gamma$
55.20 $\gamma'/(\gamma'+\gamma)$	868	56.80 $(\gamma'+\gamma)/\gamma$
55.35 $\gamma'/(\gamma'+\gamma)$	879	56.80 $(\gamma'+\gamma)/\gamma$
55.75 $\gamma'/(\gamma'+\gamma)$	907	56.90 $(\gamma'+\gamma)/\gamma$
56.25 $\gamma'/(\gamma'+\gamma)$	934	57.00 $(\gamma'+\gamma)/\gamma$
56.50 $\gamma'/(\gamma'+\gamma)$	945	57.00 $(\gamma'+\gamma)/\gamma$
57.60 $\gamma/(\gamma+\varepsilon)$	700	(66)* $(\gamma+\varepsilon)/\varepsilon$
58.00 $\gamma/(\gamma+\varepsilon)$	735	(66)* $(\gamma+\varepsilon)/\varepsilon$
58.25 $\gamma/(\gamma+\varepsilon)$	753	(66)* $(\gamma+\varepsilon)/\varepsilon$
58.45 $\gamma/(\gamma+\varepsilon)$	764	(66)* $(\gamma+\varepsilon)/\varepsilon$
58.90 $\gamma/(\gamma+\varepsilon)$	783	(66)* $(\gamma+\varepsilon)/\varepsilon$
59.75 $\gamma/(\gamma+\varepsilon)$	816	(66)* $(\gamma+\varepsilon)/\varepsilon$
59.80 $\gamma/(\gamma+\varepsilon)$	817	(66)* $(\gamma+\varepsilon)/\varepsilon$

* Not in equilibrium (comp. text).

the hexagonal phase could be identified in X-ray patterns of samples up to annealing temperatures of 1,123 K, an observation also reported by other authors[15,18]. It can therefore be assumed that in samples with less than 51 at% Se the tetragonal phase is formed during quenching. Since

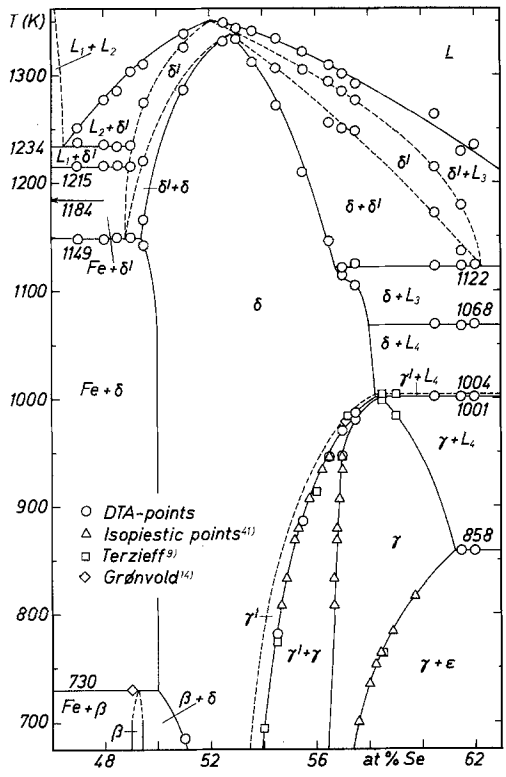

Fig. 3. Partial Iron—Selenium phase diagram (present work): ○ DTA-arrests; △ isopiestic study[41]; □ magnetic measurements[9]; ◇ *Grønvold*[14]

in the range from 20 to 49.5 at% Se DTA-measurements showed depending on the heating rate strong supercooling and superheating effects, resp., the temperature for the peritectoid decomposition of tetragonal β-FeSe into hexagonal δ-$Fe_{1-x}Se$ and α-Fe was taken from the work of *Grønvold*[14] as 730 K. Below 730 K pure tetragonal β-FeSe with PbO-structure was found between 49.0 and 49.4 at% Se. Due to the small range of homogeneity no measurable change of the lattice parameters could be observed. β-FeSe has the space group P_4/nmm—D_{4h}^7 and the lattice constants $a = 3.77_5$ and $c = 5.52_7$ Å, in good agreement with the data from literature[11, 14, 15] given in Tab. 3.

The NiAs-related structures have an extended range of homogeneity in this system. *Hägg* and *Kindström*[11] observed that the iron-rich hexagonal cell undergoes a monoclinic distortion at ≈ 53 at% Se;

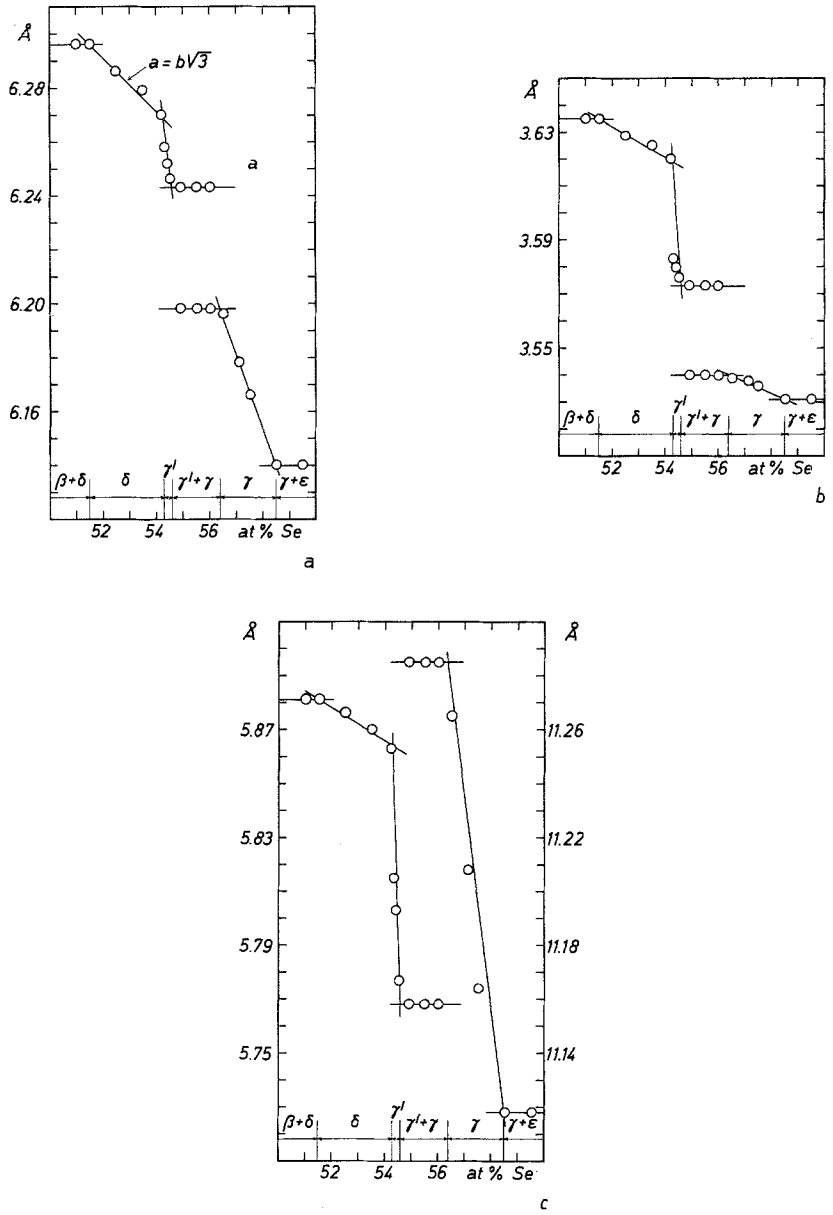

Fig. 4. Lattice parameters of the NiAs-related phases (samples quenched from 825 K; orthohexagonal orientation for the δ-phase). *a* *a*-axis, *b* *b*-axis, *c* *c*-axis

Table 3. *Lattice parameters in the iron—selenium-system*

β-Phase FeSe (PbO-Structure)

	at%Se	a, Å	c, Å
Hägg and *Kindström*[11]	ca. 50	3.765	5.518
Grønvold[14, a]	47.9	3.771-3.829	5.521-5.585
Reddy and *Chetty*[15]	51	3.77	5.53
This paper[b]	49.5	3.77_5	5.52_7

$Fe_{1-x}Se$-Phase (NiAs-like Structure)

	at%Se	a, Å	b, Å	c, Å	β, °
Hägg and *Kindström*[11]	49.1-52.5	3.637-3.607		5.958-5.844	
	53.7-60.4	6.247-6.090	3.581-3.488	5.809-5.460	90.98-91.88-90.98
Okazaki and *Hirakawa*[20]	57.1	6.167	3.537	11.17	92
Andresen[21]	57.1	6.17_2	3.53_4	11.19_5	91.51
Grønvold[14c]	53.3	3.617-3.701		5.886-5.862	
Reddy and *Chetty*[15]	51	3.61		5.93	
	60	6.26	3.59	5.82	90.98
This paper[d] δ	51.5-54.3	3.63_5-3.61_9		5.88_1-5.86_4	
γ′	54.3-54.6	6.26_9-6.24_3	3.61_9-3.57_3	5.86_4-5.76_8	91
γ′ + γ	54.6-56.4	6.24_3; 6.19_8	3.57_3; 3.54_0	5.76_8; 11.28_5	91.5
γ	56.4-58.5	6.19_8-6.14_0	3.54_0-3.53_1	11.28_5-11.11_8	92.0-91.0

ε-Phase $FeSe_2$ (Marcasite Structure)	at% Se	a, Å	b, Å	c, Å
Tengnér[12]	66.6	4.791	5.715	3.575
Fischer[29]	—	4.789	5.768	3.575
Grønvold and *Westrum*[31]	—	4.799	5.778	3.583
Kjekshus et al.[32]	—	4.8002	5.7823	3.5834
Reddy and *Chetty*[15]	66.6	4.80	5.72	3.58
This paper[d]	66.6	4.79_9	5.77_8	3.58_2

[a] Temperature: 20-440 °C. [b] Annealing temperature: 653 K. [c] Temperature: 20-495 °C. [d] Annealing temperature: 823 K.

from 53.7 to 60.4 at% Se the c-axis of the monolinic lattice changes from 5.809 to 5.460 Å. Other authors[20,21] reported at 57.1 at% Se for the c-axis double the value, i.e. 11.17 and $11.19_5^{\cdot}$ Å, resp. In the present investigation X-ray analysis of samples quenched from 653 K gave a range of homogeneity for the hexagonal δ-$Fe_{1-x}Se$-phase from 51.5 to 53.5 at% Se. In these samples the hexagonal $3c$-superstructure of the basic NiAs-lattice which has been already described by *Okazaki* and *Hirakawa*[20] could also be identified. Reflexes calculated by means of the orthohexagonal orientation could be unambiguously indexed up to diffraction angles of $\approx 30°$, and gave the lattice constants $A = \sqrt{3}\,B = 12.5$ Å, $B = 2\,a = 7{,}23$ Å, and $C = 3\,c = 17.6$ Å, in good agreement with the literature[20]. From 54 at% Se on the splitting of lines due to the monoclinic distortion could be observed. For the distorted lattice only the simple c-axis with $c' = 5.78$ Å was obtained.

Evaluation of the isopiestic experiments[41] in the range of the NiAs-related structures between 808 and 945 K pointed to the existence of a two-phase region. Since according to the phase diagrams of *Kullerud*[17] and *Svendsen*[27] the NiAs-related phase has its maximum stability range between 773 and 873 K, all further X-ray analyses were carried out with samples annealed at 823 K. Between 51.5 and 54.3 at% Se the existence of hexagonal NiAs-related δ-$Fe_{1-x}Se$ could be confirmed. In this range the lattice parameters decrease with increasing Se-content: the a-axis from 3.63_5 to 3.61_9 Å, the c-axis from 5.88_1 to 5.86_4 Å. The change of the lattice parameters with concentration is shown in Fig. 4. Tab. 3 gives a comparison of the present results with those published in the literature[11,14,15]. The Se-rich boundary of the δ-phase could be delineated in this concentration and temperature range only by X-ray analysis; it is shown in Fig. 2 and in Fig. 3 as a dashed line. Transformation between the δ- and the γ'-phase is presumably λ-type. In the narrow concentration range between 54.3 and 54.6 at% Se the X-ray patterns could be indexed assuming a monoclinically distorted structure with a simple c-axis c', since the weak reflexes [e.g. $(\bar{1}07)$, (211), (217), etc.] indicative of a doubling of the c-axis were missing. The lattice parameters of the monoclinic γ'-phase also decrease with increasing Se-content: the a'-axis from 6.26_9 to 6.24_3 Å, the b'-axis from 3.61_9 to 3.57_3 Å, and the c'-axis from 5.86_4 to 5.76_8 Å; the angle β' was found to be 91°.

Adjoining the γ'-phase a two-phase field exists between 54.6 and 56.4 at% Se with two very similar monoclinic lattices: the γ'-phase with a simple c'-axis and the γ-phase with roughly a double c-axis. Evaluation of the X-ray patterns of samples with ≈ 55.7 at% Se showed for the γ'-phase the characteristic (004)-line with an intensity comparable to that of the (008)-reflex of the γ-phase. Also for the strong reflexes $(\bar{5}13)$-$(\bar{5}16)$, (133)-(136), $(\bar{4}22)$-$(\bar{4}24)$, and so on, double instead of simple

lines could be registered. In addition X-ray films of samples with 54.8 to 56.2 at% Se contained the weak reflexes caused by doubling of the c-axis.

The (004)-line of the γ'-phase and the (008)-line of the γ-phase did not change position with increasing Se content. The (h00) and (hk0) reflexes like (600) and (330), present as broad interference bands, did not split in separate lines in *Debye-Scherrer* cameras with small diameter (57.29 mm) but showed only a shift of the maximum intensity within the interference band from smaller to larger Θ-values with increasing Se concentration. Therefore X-ray patterns of long-time annealed samples were made with *Debye-Scherrer* cameras with double diameter (114.58 mm). The broad interference bands split in two closely spaced lines which did not change position within the two-phase region. The lattice parameters of γ' and γ in this region are as follows:

γ': $a' = 6.24_3$ Å, $b' = 3.57_3$ Å, $c' = 5.76_8$ Å,
γ: $a = 6.19_8$ Å, $b = 3.54_0$ Å, $c = 11.28_5$ Å; $\beta' = \beta = 91.50°$.

All (hkl)-reflexes could be calculated with these parameters. The iron-rich and the selenium-rich boundaries of the $(\gamma' + \gamma)$-two-phase field were taken from isopiestic equilibration studies[41] and are listed in Tab. 2. At 653 K this two-phase field extends from 54.6 to 56.4 at% Se, and it becomes very small at 973 K. Just below 973 K two overlapping DTA-peaks could be registered on alloys with 57.0 and 57.5 at% Se which can be interpreted as the Fe- and the Se-rich boundary of the two-phase field. The Fe-rich boundary was confirmed by magnetic measurements[9], and the λ-transition at 57.1 at% Se and 977 K measured by *Grønvold*[14] was also on the Fe-rich side of the two-phase field. Since both the magnetic measurements[9] and the isopiestic studies[41] were indicative of a two-phase region in this part of the system, the concentration range between γ' and γ has been marked as such in Figs. 2 and 3.

Between 56.4 and 58.5 at% Se X-ray analysis of samples annealed at 823 K showed only the monoclinic γ-phase with lattice parameters decreasing with increasing Se-content: the a-axis from 6.19_8 to 6.14_0 Å, the b-axis from 3.54_0 to 3.53_1 Å, the c-axis from 11.28_5 to 11.11_8 Å, and the angle β from 92 to 91°. These values agree well with the literature[11, 15, 20, 21] and are also listed in Tab. 3 and plotted in Fig. 4. Phase boundaries determined from the breaks in the lattice parameter curves were in acceptable agreement with those derived from isopiestic measurements. The values obtained by the latter method can be considered to be more accurate.

Heating- and cooling curves from DTA-measurements of samples between 60.5 and 66.0 at% Se showed a broad peak at 1,001 K, ostensibly caused by superposition of a strong arrest at 1,001 K and a weak

arrest at 1,004 K, the former due to the peritectic decomposition of γ, the latter caused by the λ-transformation of γ' into δ. The temperature of 1,001 K agrees well with the values reported by other authors[14, 17, 27]: *Grønvold*[14] in his heat capacity measurements of Fe_3Se_4 (57.1 at% Se) found a rather broad λ-type transition with a maximum at 977 K extending towards 1,000 K which he ascribed to the transition of monoclinic into hexagonal Fe_3Se_4; *Svendsen*[27] obtained for this λ-transition a temperature of 998 K, and *Kullerud*[17] reported 1,000 K for the incongruent melting point of Fe_3Se_4.

At 66.6 at% Se the orthorhombic ε-phase $FeSe_2$ with marcasite structure was verified with the lattice constants $a = 4.79_9$ Å, $b = 5.77_8$ Å, and $c = 3.58_2$ Å, in good agreement with literature[12, 15, 29, 31, 32] (Tab. 3). The same lattice parameters for ε were found in the two-phase field ($\gamma + \varepsilon$) between 58.5 and 66.0 at% Se. Several specimens of isopiestic experiments with compositions in this region were obviously not in equilibrium. X-ray analysis of the wire specimens revealed a surface layer of $FeSe_2$ and a core of monoclinic γ. A dense non-porous layer of $FeSe_2$ apparently retarded diffusion of selenium into the interior of the specimens so that pure $FeSe_2$ was not obtained. The peritectic decomposition temperature of ε of 858 K is in good accord with other published values[16, 17, 27, 28, 33–35].

The results above 973 K are mainly based on DTA-measurements. For selenium-rich alloys agreement with literature[17, 27, 28] was quite satisfactory, on the iron-rich side and in the range of NiAs-related structures, however, observations of other authors could only be partially confirmed. Arrests at 1,145 K on the iron-rich side and at 1,108 K on the selenium-rich side of the δ-phase found by *Kullerud*[17] were also observed at 1149 and 1,122 K, resp. According to *Kullerud*[17] the arrest at 1,108 K is due to the eutectoid decomposition of a high-temperature modification of the $Fe_{1-x}Se$-phase into the δ-phase and a selenium-rich melt, and that at 1,145 K due to the peritectoid decomposition of δ into the high-temperature modification and iron (Fig. 1*a*); between these two temperatures in the range from 50 to 56 at% Se should extend the two-phase field of the δ-phase and its high-temperature modification. In spite of numerous attemps DTA-measurements failed to give any sign of a two-phase field in this temperature and concentration range. The DTA-effects in the range of the NiAs-related structures could be best explained by a maximum in the transformation temperature of the δ-phase into its high-temperature modification δ' of unknown structure at 52.8 at% Se and 1,338 K. The maximum melting point of the δ'-phase was fixed at 52.0 at% Se and 1,351 K. Both maxima were obtained by extrapolation of the corresponding curves.

On the iron-rich side of the phase diagram the eutectic between iron

and the δ'-phase at 1,215 K and 5.5 at% Se and the monotectic at 1,234 K and 46.5 at% Se with the miscibility gap ($L_1 + L_2$) extending to 6.5 at% Se are in accord with the phase diagram of *Kullerud*[17]. *Dutrizac* et al.[28] reported the monotectic temperature at $\approx$ 1,800 K. The transformation of α-Fe $\rightleftharpoons$ γ-Fe which for pure iron should occur at 1,184 K[42] could not be found thermoanalytically. On the selenium-rich side the various results published by *Kullerud*[17], *Dutrizac* et al.[28], and *Svendsen*[27] could be confirmed by DTA-measurements. In addition to the peritectic decomposition of the ε-phase at 858 K, the peritectic decomposition of the γ-phase at 1,001 K, and the λ-transformation of γ' into δ at 1,004 K which have been already mentioned above, the monotectic temperature at 1,068 K with the miscibility gap ($L_3 + L_4$) extending from 71.5 to $\approx$ 98 at% Se could be observed by thermoanalytic measurements on samples in the range between 60.5 and 66.0 at% Se.

Acknowledgment

The financial support of this investigation by the "Fonds zur Förderung der wissenschaftlichen Forschung" under grant number 2847 is gratefully acknowledged.

References

1 *K. L. Komarek* and *K. Wessely*, Mh. Chem. **103**, 896 (1972).
2 *K. L. Komarek* and *K. Wessely*, ibid. **103**, 923 (1972).
3 *K. O. Klepp* and *K. L. Komarek*, ibid. **103**, 934 (1972).
4 *K. O. Klepp* and *K. L. Komarek*, ibid. **104**, 105 (1973).
5 *H. Jelinek* and *K. L. Komarek*, ibid. **105**, 689 (1974).
6 *H. Jelinek* and *K. L. Komarek*, ibid. **105**, 917 (1974).
7 *H. Ipser*, *K. L. Komarek*, and *H. Mikler*, ibid. **105**, 1322 (1974).
8 *H. Ipser* and *K. L. Komarek*, ibid. **105**, 1344 (1974).
9 *P. Terzieff* and *K. L. Komarek*, ibid. **109**, 651 (1978).
10 *H. Sodeck*, *H. Mikler*, and *K. L. Komarek*, ibid. **110**, 1 (1979).
11 *G. Hägg* and *A. L. Kindström*, Z. phys. Chem. **B 22**, 453 (1933).
12 *S. Tengnér*, Z. anorg. allg. Chem. **239**, 126 (1938).
13 *H. Haraldsen* and *F. Grønvold*, Structure Reports **9**, 97 (1955).
14 *F. Grønvold*, Acta Chem. Scand. **22**, 1219 (1968).
15 *K. V. Reddy* and *S. C. Chetty*, Phys. Stat. Sol. (a) **32**, 585 (1975).
16 *P. Tröften* and *G. Kullerud*, Carnegie Inst. Wash. Year Book **60**, 176 (1961).
17 *G. Kullerud*, Carnegie Inst. Wash. Year Book **67** (Publ. 1969) 175 (1967—1968).
18 *A. V. Gorokh*, *L. M. Kabanova*, and *V. G. Dobosh*, Dokl. Akad. Nauk SSSR **169**, 639 (1966).
19 *T. Tsuji*, *A. T. Howe*, and *N. N. Greenwood*, J. Solid State Chem. **17**, 157 (1976).
20 *A. Okazaki* and *K. Hirakawa*, J. Phys. Soc. Japan **11**, 930 (1956).
21 *A. F. Andresen*, Acta Chem. Scand. **22**, 827 (1968).

[22] *A. Okazaki*, J. Phys. Soc. Japan **14**, 112 (1959).
[23] *A. Okazaki*, J. Phys. Soc. Japan **16**, 1162 (1961).
[24] *A. F. Andresen* and *J. Leciejewicz*, J. Physique **25**, 574 (1964).
[25] *F. Grønvold* and *E. F. Westrum, jr.*, Acta Chem. Scand. **13**, 241 (1959).
[26] *F. Grønvold*, Acta Chem. Scand. **26**, 2085 (1972).
[27] *S. R. Svendsen*, Acta Chem. Scand. **26**, 3757 (1972).
[28] *J. E. Dutrizac, M. B. I. Janjua*, and *J. M. Toguri*, Canad. J. Chem. **46**, 1171 (1968).
[29] *G. Fischer*, Canad. J. Phys. **36**, 1435 (1958).
[30] *G. S. Mann* and *L. H. van Vlack*, Met. Trans. **8B**, 47 (1977).
[31] *F. Grønvold* and *E. F. Westrum, jr.*, Inorg. Chem. **1**, 36 (1962).
[32] *A. Kjekshus, T. Rakke*, and *A. F. Andresen*, Acta Chem. Scand. **A 28**, 996 (1974).
[33] *S. R. Svendsen*, Acta Chem. Scand. **26**, 3834 (1972).
[34] *L. D. Dudkin* and *V. I. Vaidanich*, Fiz. Tverd. Tela **2**, 1526 (1960); Soviet Phys. Solid State (Engl. Transl.) **2**, 1384 (1961).
[35] *F. Grønvold*, J. Chem. Thermodynamics **7**, 645 (1975).
[36] *T. A. Bither, R. J. Bouchard, W. H. Cloud, P. C. Donohue*, and *W. J. Siemons*, Inorg. Chem. **7**, 2208 (1968).
[37] *T. Hirone, S. Maeda*, and *N. Tsuya*, J. Phys. Soc. Japan **9**, 496 (1954).
[38] *T. Hirone* and *S. Chiba*, J. Phys. Soc. Japan **11**, 666 (1956).
[39] *J. Serre* and *R. Druilhe*, C. R. Acad. Sci. Paris **B 262**, 639 (1966).
[40] *A. I. Vogel*, A Textbook of Quantitative Inorganic Analyses, 3rd ed., p. 415. London: Longmans, Green, and Co. 1966.
[41] *W. Schuster, H. Ipser*, and *K. L. Komarek*, Mh. Chem., **110**, 1171 (1979).
[42] *R. Hultgren, P. D. Desai, D. T. Hawkins, M. Gleiser, K. K. Kelley*, and *D. D. Wagman*, Selected Values of the Thermodynamic Properties of the Elements. American Society for Metals, Metals Park, Ohio (1973).